https://doi.org/10.5194/acp-2021-701
Preprint. Discussion started: 16 September 2021

Atmospheric Chemistry and Physics Discussions

Distinguishing the impacts of natural and anthropogenic aerosols on global gross primary productivity through diffuse fertilization effect

Hao Zhou [1,2], Xu Yue [3*], Yadong Lei [4], Chenguang Tian[1,2], Jun Zhu [3], Yimian Ma[1,2], Yang Cao [1,2], Xixi Yin [3], Zhiding Zhang [3]

[1] Climate Change Research Center, Institute of Atmospheric Physics (IAP), Chinese Academy of Sciences (CAS), Beijing 100029, China

[2] University of Chinese Academy of Sciences, Beijing, China

[3] Jiangsu Key Laboratory of Atmospheric Environment Monitoring and Pollution Control, Collaborative Innovation Center of Atmospheric Environment and Equipment Technology, School of Environmental Science and Engineering, Nanjing University of Information Science & Technology (NUIST), Nanjing, 210044, China

[4] State Key Laboratory of Severe Weather & Key Laboratory of Atmospheric Chemistry of CMA, Chinese Academy of Meteorological Sciences, Beijing, 100081, China

Correspondence to: Xu Yue (yuexu@nuist.edu.cn)

https://doi.org/10.5194/acp-2021-701
Preprint. Discussion started: 16 September 2021

Atmospheric Chemistry and Physics Discussions

Abstract

Aerosols can enhance ecosystem productivity by increasing diffuse radiation. Such diffuse fertilization effects (DFEs) vary among different aerosol compositions and sky conditions. Here, we apply a suite of chemical, radiation, and vegetation models in combination with ground- and satellite-based measurements to assess the impacts of natural and anthropogenic aerosol species on gross primary productivity (GPP) through DFE during 2001-2014. Globally, aerosols increase GPP by 8.9 Pg C yr^{-1} at clear skies but only 0.95 Pg C yr^{-1} at all skies. Anthropogenic aerosols account for 41% of the total GPP enhancement though they contribute only 25% to the increment of diffuse radiation. Sulfate/nitrate aerosols from anthropogenic sources make dominant contributions of 33% (36%) to aerosol DFE at all (clear) skies, followed by the ratio of 18% (22%) by organic carbon aerosols from natural sources. In contrast to other species, black carbon aerosols decrease global GPP by 0.28 (0.12) Pg C yr^{-1} at all (clear) skies. Long-term simulations show that aerosol DFE is increasing 2.9% yr^{-1} at all skies mainly because of a downward trend in cloud amount. This study suggests that the impacts of aerosols and cloud should be considered in projecting future changes of ecosystem productivity under varied emission scenarios.

Keywords: Diffuse fertilization effect, gross primary productivity, anthropogenic aerosols, natural aerosols, YIBs model

https://doi.org/10.5194/acp-2021-701
Preprint. Discussion started: 16 September 2021

1 Introduction

Diffuse light enhances plant photosynthesis more efficiently than direct light (Gu et al., 2002;Alton et al., 2007;Mercado et al., 2009;Jing et al., 2010;Cirino et al., 2014;Zhou et al., 2021b;Zhou et al., 2021c). The cause for such difference is that diffuse light can penetrate into the deep canopy and enhance light use efficiency (LUE=GPP/PAR, gross primary production per photosynthetically active radiation) of shaded leaves (Roderick et al., 2001;Gu et al., 2003;Rap et al., 2015). However, direct light is absorbed only by sunlit leaves and much of it is wasted because these leaves are usually at the light saturated conditions (Gu et al., 2002;He et al., 2013). As a result, increasing the diffuse radiation can help promote canopy photosynthesis through the diffuse fertilization effect (DFE).

Atmospheric aerosols can alter the quality of sunlight reaching Earth's surface by absorbing and scattering solar insolation (Zhou et al., 2021a). The aerosol-induced radiative impacts on terrestrial ecosystem productivity have been investigated in both observational and modeling studies (Table 1). Observations found unexpected decline of atmospheric carbon dioxide in 1990s, which was attributed to the increase of vegetation carbon uptake owing to the massive eruption of Mt. Pinatubo in 1991 (Roderick et al., 2001). Sulfate aerosols from volcanic eruption almost doubled diffuse radiation at the clear sky, leading to the enhancement of plant productivity by 23% at Harvard forests in 1992 (Gu et al., 2003). With the development of ground-based instruments and satellite remote sensing, more observational data have been applied to detect the aerosol DFE. Strada et al. (2015) estimated aerosol DFE on plant productivity

https://doi.org/10.5194/acp-2021-701
Preprint. Discussion started: 16 September 2021

using aerosol optical depth (AOD) from satellite cloudless observations at 10 flux sites, and found that aerosols enhance GPP by 13% in midday hours under high AOD conditions (>0.4) for deciduous and mixed forests. Similarly, Ezhova et al. (2018) found that aerosols increase clear-day diffuse fraction from 0.11 to 0.27 at five remote sites in Eurasia, leading to the enhancement of site-level GPP by 6-14%.

In contrast to the large benefits at clear days, the aerosol DFE is limited at cloudy days. Kanniah et al. (2013) explored cloud direct radiative effects on canopy productivity using observed carbon fluxes and radiation in tropical savannas, and found that thick cloud masked aerosol DFE and reduced GPP by 26%. Cirino et al. (2014) also found that aerosol DFE cannot increase plant photosynthesis under cloudy conditions. These studies indicated that aerosol DFE is subject to sky conditions and aerosol loading, because the potential benefits from DFE can be offset or even reversed by simultaneous reductions in direct radiation caused by thick cloud or high aerosol loading (Alton, 2008;Cirino et al., 2014;Yue and Unger, 2017;Zhou et al., 2021a).

Although observational studies directly estimate site-level aerosol DFE, they are not able to reveal regional or global aerosol DFE due to the limited spatiotemporal coverage. On the global scale, studies using varied models showed that aerosol DFE enhances global GPP by 4.9 Pg C yr^{-1} (Chen and Zhuang, 2014), 1-2% (Strada and Unger, 2016) and 1.0±0.2 Pg C yr^{-1} (Yue and Unger, 2018) at different periods. Rap et al. (2018) specifically explored DFE from biogenic aerosols and found that biogenic aerosols enhance global NPP by 1.23 Pg C yr^{-1}. Regionally, Matsui et al. (2008) applied a land surface model and estimated that aerosol DFE decreased net primary production (NPP)

https://doi.org/10.5194/acp-2021-701
Preprint. Discussion started: 16 September 2021

by 0.09% in 2000 but increased NPP by 0.5% in 2001 over eastern U.S., because the cloud optical depth was about half in 2001 relative to 2000. At the same region, Keppel-Aleks and Washenfelder (2016) estimated sulfate aerosol DFE using Community Earth System Model and found that the reductions of sulfate aerosols by 3.0±0.6% yr^{-1} led to reductions of 0.6% yr^{-1} in diffuse radiation and 0.07% yr^{-1} in regional GPP during 1995-2013. In Amazon, fire aerosols are estimated to play varied DFEs among different studies (Rap et al., 2015;Moreira et al., 2017;Yue and Unger, 2018;Malavelle et al., 2019). For example, Rap et al. (2015) found that fire aerosols enhance NPP by 1.4-2.8% while Moreira et al. (2017) estimated that fire aerosols enhance GPP by 27%. Such differences are mainly attributed to the high aerosol loading in Moreira et al. (2017) for September 2010, but much lower loading in Rap et al. (2015) for the 10-year (1998-2007) averages. Although these studies assessed the DFE of total aerosols or the specific species (e.g., sulfate, fire, or biogenic), the individual DFEs of natural and anthropogenic aerosols on global terrestrial productivity remain unclear.

In this study, we explore the impacts of natural and anthropogenic aerosol DFE on global GPP during 2001-2014 using both multi-source observations and a series of well-validated models. A chemical transport model (CTM) is used to predict changes of natural and anthropogenic aerosol concentrations. A radiative transfer model is applied to calculate the perturbations in direct and diffuse PAR caused by aerosols. A global dynamic vegetation model is used to quantify changes of global GPP caused by aerosol DFE. The main objectives are (1) to distinguish the DFEs of natural and anthropogenic aerosols on global GPP and (2) to explore the different characteristics of aerosol DFEs

https://doi.org/10.5194/acp-2021-701
Preprint. Discussion started: 16 September 2021

for varied species.

2 Methods

2.1 Chemical transport model

The Goddard Earth Observing System coupled with Chemistry (GEOS-Chem, http://geos-chem.org) is a three-dimensional (3-D) CTM for simulating atmospheric compositions and air quality (Bey et al., 2001). Global anthropogenic emissions during 2001-2014 are from the Community Emissions Data System (CEDS) inventory (http://www.globalchange.umd.edu/ceds/). The CEDS inventory has been used as anthropogenic emissions in the Coupled Model Intercomparison Project Phase 6 (CMIP6), and this emission database relies on existing energy consumption datasets and regional or country-specific inventories to produce trends over recent decades (Hoesly et al., 2018). The specific emission species include aerosols (black carbon, organic carbon), aerosol precursors and reactive compounds (SO_2, NO_x, NH_3, CH_4, CO, and non-methane volatile organic compounds (VOCs)) (Supplementary Table 1). To estimate modeling uncertainties due to emission inventories, the Emissions Database for Global Atmospheric Research (EDGAR) inventory vision 4.3.1 (https://edgar.jrc.ec.europa.eu/) during 2001-2010 is also used as alternative anthropogenic emissions for GEOS-Chem model. For natural emissions, the Global Fire Emission Database (GFED) version 4 inventory is used to represent emissions from open fires (http://www.globalfiredata.org/). Biogenic VOC emissions are calculated using the Model of Emissions of Gases and Aerosols from Nature (MEGAN

https://doi.org/10.5194/acp-2021-701
Preprint. Discussion started: 16 September 2021

v2.1) (Guenther et al., 2012). Natural emissions of sea salt (Jaeglé et al., 2011), dimethyl sulfate (Breider et al., 2017), volcanic SO_2 (Fisher et al., 2011) and NH_3 are from the Global Emissions InitiAtive (GEIA, http://www.geiacenter.org/). In this study, GEOS-Chem version 12.0.0 is used to simulate concentrations of natural and anthropogenic aerosols at a horizontal resolution of 4˚×5˚ and 47 vertical layers. The CTM is driven with assimilated meteorology from the Modern-Era Retrospective analysis for Research and Applications, version 2 (MERRA2).

2.2 Radiative transfer model

The Column Radiation Model (CRM) is the standalone version of the radiative transfer module used by the NCAR Community Climate Model (http://www.cesm.ucar.edu/models/). In this model, aerosol direct radiative effects including absorbing and scattering processes are calculated at 20 vertical layers from surface to 0.5 hPa at hourly intervals (Yue and Unger, 2017). The CRM utilizes aerosol profiles of all species simulated by GEOS-Chem, including sulfate, nitrate, black carbon (BC), organic carbon (OC), dust (clay and silt) and sea salt (coarse and accumulation modes). Aerosol optical parameters (e.g. single scattering albedo, extinction coefficients, and asymmetric parameters) are adopted from Yue and Liao (2012) for sea salt, Yue et al. (2010) for mineral dust, and the RegCM4 model for other species (Giorgi et al., 2012). In this study, the CRM is used to simulate aerosol-induced perturbations in surface radiative fluxes including diffuse and direct PAR. The model is driven with hourly 1˚×1˚ meteorology from MERRA-2 reanalyses, and 3-hourly

https://doi.org/10.5194/acp-2021-701
Preprint. Discussion started: 16 September 2021

cloud cover and liquid water path from CERES SYN1deg (http://ceres.larc.nasa.gov).

2.3 Dynamic vegetation model

The Yale Interactive terrestrial Biosphere (YIBs) model is a process-based vegetation model that dynamically simulates tree growth and leaf area changes (Yue and Unger, 2015). The model uses the well-established leaf photosynthesis (Farquhar et al., 1980) and stomatal conductance schemes (Ball et al., 1987). The canopy is divided into sunlit and shaded portions to separate photosynthetic responses to diffuse and direct light (Spitters et al., 1986). We distinguish light absorption between sunlit (receiving both diffuse and direct light) and shaded leaves (receiving only diffuse light), and derive canopy photosynthesis as the sum of that from sunlit and shaded leaves:

$$A_{total} = A_{sunlit} \times F_{sunlit} + A_{shaded} \times (1 - F_{sunlit}) \quad (1)$$

where A_{sunlit} and A_{shaded} are the photosynthesis of sunlit and shaded leaves, respectively. The fraction of sunlit leaf area F_{sunlit} is calculated as:

$$F_{sunlit} = e^{-kL} \quad (2)$$

Here, L is leaf area index (LAI) at one canopy layer and k is extinction coefficient defined as $0.5/cos\alpha$ (solar zenith α).

Simulated GPP by YIBs model were validated using ground-based observations at 145 sites and yielded an average correlation coefficient of 0.76 for all sites (Yue and Unger, 2015). The simulated global GPP also shows reasonable spatiotemporal variations compared with satellite retrievals (Yue et al., 2015). Recently, the model joined the multi-model ensemble project of TRENDY to provide the estimates of global

https://doi.org/10.5194/acp-2021-701
Preprint. Discussion started: 16 September 2021

carbon budget (Friedlingstein et al., 2020). In this study, the YIBs is used to isolate impacts of aerosol-induced PAR changes on GPP on the global scale. The model is driven with 1°×1° meteorological forcing from MERRA-2 reanalyses and PAR (both diffuse and direct) simulated by CRM model.

2.4 Model simulations

We perform 2 GEOS-Chem runs, as well as 22 CRM and YIBs runs to isolate aerosol direct radiative impacts on GPP at different sky conditions (Supplementary Table 2). The GEOS-Chem runs GC_ALL and GC_NAT are driven with the same meteorology and emissions except that the former includes all source of emissions while the latter excludes anthropogenic emissions. The differences between GC_ALL and GC_NAT represent aerosol concentrations contributed by anthropogenic sources. Both GC_ALL and GC_NAT runs provide 3-D concentrations of different aerosol types including sulfate, nitrate, OC, BC, dust and sea salt. The CRM runs aim to calculate aerosol-induced PAR changes using aerosol profiles simulated by GEOS-Chem. These runs can be divided into two groups, with CLD runs (all-sky conditions) forced with observed cloud profiles while CLR runs (clear-sky conditions) forced without any cloud coverage. CRM_ALL and CRM_NAT are driven with aerosol profiles of all species from GC_ALL and GC_NAT, respectively. The impacts of individual aerosol species on PAR are isolated with individual aerosol profiles from either GC_ALL or GC_NAT. For example, OC from GC_ALL and cloud amounts from CERES SYN1deg are used to drive CRM (CRM_ALL_OCCLD) so as to isolate the impacts of OC aerosols on PAR

https://doi.org/10.5194/acp-2021-701
Preprint. Discussion started: 16 September 2021

at all-sky conditions. For each of CRM runs, the predicted diffuse and direct PAR are used as input for YIBs model to simulate GPP changes caused by aerosol DFEs.

2.5 Observations for model evaluations

We use site-level measurements of carbon fluxes from the FLUXNET2015 product (http://fluxnet.fluxdata.org/) to validate model GPP and its responses to diffuse/direct radiation. We select 10 sites providing simultaneous observations of diffuse radiation and GPP at half-hourly time interval for at least 8 years. On the global scale, observed AOD is retrieved from the Moderate Resolution Imaging Spectroradiometer (MODIS, https://modis.gsfc.nasa.gov) and GPP is derived using global OCO-2-based SIF product (Li and Xiao, 2019). The all-sky and clear-sky shortwave radiation are adopted from CERES SYN1deg (http://ceres.larc.nasa.gov) to validate the CRM radiative transfer model.

3 Results

3.1 Model evaluations

The YIBs model simulates reasonable spatial pattern of GPP compared to observations (Figure S1) with a high correlation coefficient (R) of 0.88 (p<0.01) and a low normalize mean bias (NMB) of -2.3%. Similarly, modeled AOD from GEOS-Chem model reproduces the observed spatial pattern from MODIS product with high R of 0.78 (p<0.01), though overestimates the mean AOD by 21.7% in eastern China and 37.9% in southern Africa while underestimates AOD by 35.7% in Amazon, 25.2% in

https://doi.org/10.5194/acp-2021-701
Preprint. Discussion started: 16 September 2021

Central Africa and 53.4% in southeast Asia, leading to a global NMB of -25.8%.

The CRM model driven with aerosol concentrations from GEOS-Chem shows similar patterns of shortwave radiation to the satellite observations (Figure S2). The simulations match observations well with high R of 0.98 and low NMB of 4.1% at all-sky conditions, and show even better performance with R of 1 and NMB of 3.7% at clear skies. Moreover, the CRM model simulates reasonable aerosol direct radiative effects compared to multiple radiative transfer models as shown in Yue and Unger (2018).

We then compared the simulated and observed GPP responses to direct (diffuse fraction <0.2) and diffuse radiation (diffuse fraction >0.8) (Figure 1). Observations and simulations show that diffuse light can increase GPP more efficiently than direct radiation as shown by the higher GPP-PAR slopes at diffuse conditions. Similar results were achieved by Mercado et al. (2009) and Yue and Unger (2018) using the same methods. The diffuse fertilization efficiency, percentage changes in GPP per unit diffuse PAR, is estimated to be 0.45-0.7% W^{-1} m^2 for observations and 0.3-0.69% W^{-1} m^2 for simulations. As a result, the YIBs model can reasonably reproduce varied light-response curves so as to isolate GPP responses to direct and diffuse radiation.

3.2 Changes of PAR by aerosols

Appearance of aerosols on average decreases total surface PAR by 1.52 W m^{-2} at all skies and 2.73 W m^{-2} at clear skies on the global scale. Under all-sky conditions, aerosols increase diffuse PAR by 1.26 W m^{-2} (Figure 2a) but decrease direct PAR by

https://doi.org/10.5194/acp-2021-701
Preprint. Discussion started: 16 September 2021

2.78 W m^{-2} (Figure S3a). These changes are larger in clear-sky conditions with increase of diffuse PAR by 4.98 W m^{-2} (Figure 2d) and decrease of direct PAR by 7.71 W m^{-2} (Figure S3d). The cause of smaller PAR changes at all skies is that cloud tends to weaken aerosol radiative forcing by amplifying absorption and diminishing scattering (Paulot et al., 2018).

At all-sky conditions, natural aerosols dominate aerosol-induced PAR changes by increasing diffuse PAR of 0.93 W m^{-2} (Figure 2b) and decreasing direct PAR of 2.05 W m^{-2} (Figure S3b). As a comparison, anthropogenic aerosols induce much smaller changes of diffuse radiation by 0.33 W m^{-2} and direct radiation of -0.72 W m^{-2} (Figures 2c and S3c). Natural aerosols mainly influence PAR fluxes in northern Africa owing to large amount of dust aerosols, while anthropogenic aerosols dominate PAR changes in eastern China, India, and eastern U.S due to the large anthropogenic emissions. At clear-sky conditions, natural aerosols increase diffuse PAR by 3.79 W m^{-2} (Figure 2e) and decrease direct PAR by 5.84 W m^{-2} (Figure S3e), and anthropogenic aerosols on average increase diffuse PAR by 1.19 W m^{-2} and decrease direct PAR by 1.88 W m^{-2}.

We further explore the contributions of individual aerosol species to the changes of diffuse and direct PAR at all skies (Figures S4 and S5). On the global scale, sulfate and nitrate aerosols increase diffuse PAR by 0.57 W m^{-2}, accounting for 51% of aerosol-induced diffuse PAR changes. Meanwhile, diffuse PAR is increased 0.05 W m^{-2}, 0.37 W m^{-2} and 0.25 W m^{-2} by the scattering effects of OC, dust, and sea salt aerosols. However, BC aerosols reduce diffuse PAR by 0.06 W m^{-2} due to the strong absorption. The changes of direct PAR caused by all aerosol species are negative, especially that

https://doi.org/10.5194/acp-2021-701
Preprint. Discussion started: 16 September 2021

by sulfate and nitrate (-0.97 W m^{-2}), dust (-0.86 W m^{-2}), and sea salt (-0.5 W m^{-2}). Generally, natural aerosols dominate changes of diffuse and direct PAR owing to the large contributions from dust and sea salt aerosols. However, sulfate, nitrate, and BC aerosols from anthropogenic sources dominate the changes of diffuse and direct PAR over eastern China, Indian and eastern U.S.

3.3 DFE by natural and anthropogenic aerosols

We quantify the percentage changes of global GPP caused by aerosol DFE. On the global scale, aerosol DFE increases GPP by 0.65 % (0.95 ± 0.13 Pg C yr^{-1}) at all skies (Figure 3a). Relatively high enhancements (>2%) in GPP are found over middle latitudes (20-50˚N) following the changes of diffuse PAR (Figure 2a). The DFE of natural aerosols increases global GPP by 0.38% (0.56 ± 0.1 Pg C yr^{-1}), mainly over Middle East and northern Africa due to dust aerosols (Figure S6a and S7g). The DFE of anthropogenic aerosols increases global GPP up to 0.27 % (0.39 ± 0.04 Pg C yr^{-1}), especially over populous regions including northeast China, Middle East and contiguous U.S (Figure S6b).

At clear skies, aerosol DFE increases global GPP up to 7.8% (8.91 ± 0.26 Pg C yr^{-1}) (Figure 3c), which is around 9.5 times of that at all skies (Figure 3a). In most regions, aerosol DFE increases GPP by more than 4%, with the maximum enhancement of 22.7% in East Asia. The DFE of natural aerosols enhances global GPP by 4.6%, with large changes over Amazon, center Africa, boreal Asia, and North America (Figure S6c). Meanwhile, anthropogenic aerosols increase GPP by 3.2%, mainly located at eastern

https://doi.org/10.5194/acp-2021-701
Preprint. Discussion started: 16 September 2021

U.S, Europe, boreal Asia, India and East Asia (Figure S6d).

We further quantify the contributions of anthropogenic aerosols to the total aerosol DFE. Although cloud masks aerosol DFE and significantly reduces GPP enhancement, the contributions of anthropogenic aerosols remain similar between all-sky (Figure 3b) and clear-sky (Figure 3d) conditions. Relatively high contributions (>50%) are located at low-mid latitudes including North America, Europe, and eastern China. Low contributions (<50%) are found at other regions such as Africa, South America, and Australia. On the global scale, anthropogenic aerosols on average contribute to 41% of the total aerosol DFE at all-sky conditions (Figure S6a and S6b). Anthropogenic aerosols dominate DFE over 30.5% of land grids at all skies, but only 19.5% at clear skies (Figure 3b and 3d). The most significant differences are located at boreal Europe where the anthropogenic aerosols make dominant contributions to DFE at clear skies while the natural species dominate at all skies.

3.4 DFE by individual aerosol species

We isolate the DFE of individual aerosol species on global GPP (Figures S7 and S8). At all-sky conditions, sulfate and nitrate aerosols averagely increase GPP by 0.79 Pg C yr^{-1}, to which anthropogenic sources contribute 0.58 Pg C yr^{-1} (Figure S7f). OC aerosols increase global GPP by 0.47 Pg C yr^{-1}, to which natural sources contribute 0.32 Pg C yr^{-1} (Figure S7c). As the dominant natural species, dust and sea salt are generated from non-vegetated areas. They can increase GPP of downwind land regions by 0.17 Pg C yr^{-1} (Figure S7g) and 0.06 Pg C yr^{-1} (Figure S7h), respectively. Different from the

https://doi.org/10.5194/acp-2021-701
Preprint. Discussion started: 16 September 2021

above species, BC aerosols lead to negative impacts on GPP up to -0.28 Pg C yr^{-1} globally due to the strong absorbing radiative effects. Regionally, such negative effects are prominent over center Africa from biomass burning (Figure S7a) and eastern China from anthropogenic emissions (Figure S7b).

At clear-sky conditions, scattering aerosols show larger DFE compared to the all-sky conditions. sulfate and nitrate aerosols increase global GPP by 5.18 Pg C yr^{-1}, which is 6.6 times of that at all skies. The DFE of OC aerosols also largely increase to 2.89 Pg C yr^{-1}, in which 2.21 Pg C yr^{-1} is from natural sources. Dust and sea salt aerosols lead to positive impacts on global GPP by 1.32 Pg C yr^{-1} and 0.48 Pg C yr^{-1}, respectively. In contrast, BC aerosols reduce global GPP by 0.12 Pg C yr^{-1}, much weaker than the magnitude of 0.28 Pg C yr^{-1} at all skies. Such change manly follows the larger diffuse absorption by BC aerosols at all skies (0.06 W m^{-2}) than that at clear skies (0.02 W m^{-2}).

We then identify the aerosol species making the dominant contributions to the total aerosol DFE (Figure 4). At all-sky conditions, sulfate and nitrate aerosols lead the DFE at 65% grids (Figure 4a) and account for 44.7% of the total absolute GPP changes (Figure 4c). The secondary contribution is from OC aerosols, which account for 26.7% of the total DFE. Dust and sea salt aerosols contribute to the total DFE by 9.5% and 3.4%, respectively (Figure 4c). BC aerosols exert negative DFE, the absolute value of which is equivalent to 15.8% of the total DFE. Regionally, sulfate and nitrate aerosols lead DFE in eastern China, India, eastern U.S., and Europe, while dust aerosols dominate DFE at Middle East (Figures 4e and 4f). At clear-sky conditions, the

https://doi.org/10.5194/acp-2021-701
Preprint. Discussion started: 16 September 2021

percentage contributions of sulfate and nitrate aerosols to the total DFE further increase to 51.8% on the global scale (Figure 4d). OC, dust, and sea salt aerosols show comparable contributions to DFE as that at all skies. However, the absolute ratios by BC aerosols significantly reduce to 1.2%, because BC-induced DFE is limited while DFE of other species is significantly strengthened at clear skies (Figure S8).

We further explore the interannual variations of GPP changes caused by aerosol DFE from natural and anthropogenic sources (Figure 5). At all-sky conditions, aerosol DFE significantly ($p < 0.05$) increases by 2.89% yr^{-1} (24.6 Tg C yr^{-2}) on the global scale (Figure S9a). Such enhancement is mainly located in northeastern China, India, central Africa, and Europe (Figure S10a). Natural aerosols lead to a positive trend of 4.7% yr^{-1} in the global GPP (22 Tg C yr^{-2}), which is six times of the trend of 0.67% yr^{-1} (2.6 Tg C yr^{-2}) from anthropogenic aerosols (Figure 5a). At clear-sky conditions, aerosol DFE increases by only 0.4% yr^{-1} (Figure S9b), much lower than that at all skies (Figure S9a). Both the DFE trends from natural and anthropogenic aerosols are limited (Figure 5b). The contrast of DFE trends between different sky conditions is related to the changes of cloud amount, which shows a significant reduction trend of 0.38% yr^{-1} in 2001-2014 (Figure S9c), especially over Amazon and eastern U.S. (Figure S10d). The reduction of cloud helps increase or maintain aerosol DFE at all-sky conditions (Figure S10c). The trend of all-sky aerosol DFE is mainly contributed by dust aerosols from natural sources, which increases by 4.75% yr^{-1} during 2001-2014 (Figure 5c). The trend of clear-sky aerosol DFE is mainly attributed to sulfate and nitrate aerosols, which increase by 0.44% yr^{-1} during 2001-2014 (Figure 5d).

https://doi.org/10.5194/acp-2021-701
Preprint. Discussion started: 16 September 2021

4 Discussion

4.1 Factors influencing aerosol DFE

We quantified the impacts of sky conditions, emission sources, and aerosol species on terrestrial ecosystem productivity through aerosol DFE. In our simulations, aerosols increase global GPP by 8.91 Pg C yr^{-1} at clear skies but only 0.95 Pg C yr^{-1} at all skies. Similarly, Cohan et al. (2002) and Yue and Unger (2017) found aerosol DFE was limited at cloudy skies. Cloud can mask aerosol DFE by modifying both the quantity and quality of aerosol radiative perturbations (Yu et al., 2006). First, cloud weakens the impacts of aerosols on both direct and diffuse radiation (Figure 2 and S3) by reducing the total sunlight available for the extinction by aerosols (Kinne, 2019). Therefore, the smaller changes in diffuse PAR by aerosols at all skies (Figure 2) result in lower DFE than that at clear skies. Second, cloud significantly reduces direct radiation and limits the potential of increasing GPP by diffuse radiation. Observations have shown an optimal diffuse fraction of 0.4-0.6 to enhance GPP for most plant types (Zhou et al., 2021c). A further increase of diffuse fraction above the optimal range will dampen GPP due to the reduced photosynthesis of sunlit leaves. Appearance of cloud has provided an environment with high diffuse fraction that aerosols may have limited benefits or even negative effects for GPP (Yue and Unger, 2017). Such relationship also explains why the decreasing trend of global cloud amount contributes to an increased aerosol DFE (Figure 5a).

Anthropogenic aerosols account for ~25% of the total aerosol-induced

https://doi.org/10.5194/acp-2021-701
Preprint. Discussion started: 16 September 2021

enhancement of diffuse radiation (Figure 2), while they contribute 41% to the total aerosol DFE at both all and clear sky conditions (Figure 3). The higher efficiency of anthropogenic aerosols in increasing GPP is partly associated with their geographic distribution. Regionally, anthropogenic aerosols take a leading role in DFE over North America, Europe, India, and eastern China, consistent with the estimations by Strada and Unger (2016). On the other hand, natural aerosols dominate DFE at the tropical regions. Observations have revealed higher optimal diffuse fraction at higher latitudes, where the higher solar zenith angle induces larger fraction of shading leaves (Zhou et al., 2021c). As a result, the same amount of diffuse radiation increased by anthropogenic aerosols results in higher GPP enhancement at the middle latitudes than natural aerosols at low latitudes. Furthermore, a dominant fraction of natural aerosols is contributed by dust and sea salt, which increase diffuse radiation over the barren land or open ocean with little forest coverage (Figure 2). In contrast, most anthropogenic aerosols locate at populous regions covered with dense vegetation. Consequently, the diffuse radiation by anthropogenic aerosols has more interactions with ecosystems than that from natural sources.

Different aerosol species induce varied DFEs to global GPP. Sulfate and nitrate dominate the aerosols-induced GPP changes (Figure 4) because their strong scattering effects (Gu et al., 2003) largely increase diffuse radiation (Figure S7 and S8). Keppel-Aleks and Washenfelder (2016) estimated that the regional reductions of sulfate aerosols decreased diffuse radiation by 0.6% yr^{-1} and GPP by 0.07% yr^{-1} in eastern U.S. during 1995-2013. Such negative trends of GPP can also be found over the same region

https://doi.org/10.5194/acp-2021-701
Preprint. Discussion started: 16 September 2021

in our clear-sky simulations (Figure S10b). However, the global ΔGPP shows limited trends at clear skies (Figure 5b) because the enhanced SO_2 emissions in China at the same period (Hoesly et al., 2018) increased sulfate loading, promoted local GPP (Figure S10b), and offset the negative ΔGPP in eastern U.S. In our simulations, OC aerosols promote global GPP by 0.47 Pg C yr^{-1}. Such magnitude is much lower than the estimates of 0.76-1.61 Pg C yr^{-1} for the same aerosol species by Rap et al. (2018). The main cause of such discrepancy is related to the predicted aerosol concentrations and radiative effects in two studies (Zhou et al., 2021a). Dust and sea salt aerosols increase regional GPP over arid and coastal regions due to the large local emissions (Yue et al., 2010;Yue and Liao, 2012). At all skies, dust exerts a large DFE over North Africa and Middle East (Figure 3a) because of the low cloud coverage (Figure S11). However, such high GPP ratio shows limited contributions (Figure 4) to global total ΔGPP because of the extremely low baseline GPP in arid regions. Different from above species, BC exerts negative impacts on direct and diffuse PAR owing to strong absorbing properties (Kvalevåg and Myhre, 2007). As a result, BC aerosols always decrease GPP with stronger dampening effects at all skies (Figures 4c and 4d) when the light availability is much smaller than that at clear skies.

4.2 Uncertainties

Our simulations are subject to limitations and uncertainties. First, biases in aerosol profiles may influence the derived aerosol DFE. We used the chemical transport model GEOS-Chem to predict aerosol concentrations and identify contributions from natural

https://doi.org/10.5194/acp-2021-701
Preprint. Discussion started: 16 September 2021

and anthropogenic sources. Evaluations showed that GEOS-Chem underestimated global AOD by 25.8%, especially over Amazon, central Africa, and boreal Asia (Figure S1) where natural aerosols dominate. Such bias in part explains why Rap et al. (2018) estimated that biogenic aerosols increased global NPP by 1.23 Pg C yr^{-1} with hotspots over Amazon and central Africa, while our study derived only a moderate enhancement of 0.32 Pg C yr^{-1} by natural OC aerosols. In contrast, simulated AOD is overestimated in eastern China where anthropogenic sources dominate. In this study, CEDS emission inventory is used for anthropogenic emissions. Here, we used another emission database (EDGAR) to assess the uncertainties of DFE from anthropogenic aerosols. The new simulations showed that anthropogenic aerosols increased global GPP by 0.31 Pg C yr^{-1} (Figures S12-S13), lower than the value of 0.39 Pg C yr^{-1} predicted with CEDS inventory (Figure 3). The spatial patterns of dominant species for aerosol DFE (Figure S14) remain similar to that from CEDS under both sky conditions.

Second, uncertainties in the radiative transfer may cause biases to aerosol DFE. Although the CRM was fully validated with observations (Figure S2), simulated aerosol radiative effects showed large differences compared to other studies. For example, Chen and Zhuang (2014) found that aerosols increased surface diffuse PAR by 5.2 W m^{-2} using another radiative transfer model. In our simulations, we estimated that aerosols increased diffuse PAR by only 1.26 W m^{-2}. As a result, the GPP enhancement by aerosol DFE is 0.95 ± 0.13 Pg C yr^{-1} in our study, much lower than the value of 4.9 Pg C yr^{-1} in Chen and Zhuang (2014) though the latter study also considered aerosol-induced changes in temperature and soil moisture. However, the aerosol radiative effects are

https://doi.org/10.5194/acp-2021-701
Preprint. Discussion started: 16 September 2021

likely overestimated in Chen and Zhuang (2014), which predicted total (direct + diffuse) reductions of 21.9 W m^{-2} in surface solar radiation by aerosols; such magnitude is much higher than the multi-model ensemble estimate of -6.3 W m^{-2} at clear skies (Yu et al., 2006). As a comparison, our simulations showed a reduction of 5.8 W m^{-2} in surface shortwave radiation, much closer to the ensemble estimates by Yu et al. (2006).

Third, we neglected the climatic responses to aerosol radiative effects. Surface temperature and relative humidity is altered in response to radiative changes caused by aerosols (Jing et al., 2010;Cirino et al., 2014). The increase of relative humidity can increase plant photosynthesis owing to the enhancement of water use efficiency (Lu et al., 2017;Wang et al., 2021), but the impacts of cooling on photosynthesis are dependent on whether local background temperature is over the optimal temperature (Farquhar et al., 1980). Moreover, the changes in cloud from aerosol indirect effects were not considered in this study. Cloud can significantly influence aerosol DFE because of its strong scattering effects (Figure 3). The perturbations in cloud can further influence surface temperature, precipitation, and radiation (Zhu et al., 2019), leading to more complex impacts on terrestrial ecosystem productivity. However, these interactive effects by aerosols need to be resolved using earth system models that implement fully coupled atmospheric chemistry, radiation, land biosphere, and climate feedbacks.

4.3 Implications

Our study reveals that aerosol DFE can enhance global GPP by 0.95 Pg C yr^{-1} at all skies and as high as 8.91 Pg C yr^{-1} at clear skies. The natural and anthropogenic

https://doi.org/10.5194/acp-2021-701
Preprint. Discussion started: 16 September 2021

aerosols make comparable contributions globally but with distinct spatial patterns. The DFE, as well as the climatic effects, suggests that aerosols play important roles in mitigating global warming through direct (cooling) and indirect (more carbon assimilation) processes. Although the reductions of aerosols may weaken the DFE, the associated reductions of cloud amount due to reduced aerosol-cloud interactions may induce more benefits to ecosystems. Furthermore, reductions of black carbon aerosols help relieve both climate warming and GPP inhibitions. Our results suggest that aerosol DFE should be considered in projecting future changes in terrestrial ecosystem productivity especially for different emission scenarios.

Acknowledgements

This work was jointly supported by the National Key Research and Development Program of China (grant no. 2019YFA0606802) and Jiangsu Science Fund for Distinguished Young Scholars (grant no. BK20200040).

Data availability

The simulated GPP and diffuse PAR caused by natural and anthropogenic aerosols on this paper are publicly available via Zenodo (http://doi.org/10.5281/zenodo.5115314).

Author contributions

X.Y. conceived the study; X.Y., H.Z. and Y.D.L. designed the research and performed simulations; H.Z. completed data analysis and the first draft; X.Y. reviewed and edited the manuscript; C.G.T, J.Z., Y.M.M., Y.C. X.X.Y and Z.D.Z were responsible for data collection processes.

https://doi.org/10.5194/acp-2021-701
Preprint. Discussion started: 16 September 2021

Competing interests

The authors declare no competing interests.

https://doi.org/10.5194/acp-2021-701
Preprint. Discussion started: 16 September 2021

Reference:

Alton, P. B., North, P. R., and Los, S. O.: The impact of diffuse sunlight on canopy light-use efficiency, gross photosynthetic product and net ecosystem exchange in three forest biomes, Global Change Biology, 13, 776-787, 10.1111/j.1365-2486.2007.01316.x, 2007.

Alton, P. B.: Reduced carbon sequestration in terrestrial ecosystems under overcast skies compared to clear skies, Agricultural and Forest Meteorology, 148, 1641-1653, https://doi.org/10.1016/j.agrformet.2008.05.014, 2008.

Ball, J. T., Woodrow, I. E., and Berry, J. A.: A Model Predicting Stomatal Conductance and its Contribution to the Control of Photosynthesis under Different Environmental Conditions, in: Progress in Photosynthesis Research: Volume 4 Proceedings of the VIIth International Congress on Photosynthesis Providence, Rhode Island, USA, August 10–15, 1986, edited by: Biggins, J., Springer Netherlands, Dordrecht, 221-224, 1987.

Bey, I., Jacob, D. J., Yantosca, R. M., Logan, J. A., Field, B. D., Fiore, A. M., Li, Q. B., Liu, H. G. Y., Mickley, L. J., and Schultz, M. G.: Global modeling of tropospheric chemistry with assimilated meteorology: Model description and evaluation, J Geophys Res-Atmos, 106, 23073-23095, 10.1029/2001jd000807, 2001.

Breider, T. J., Mickley, L. J., Jacob, D. J., Ge, C., Wang, J., Payer Sulprizio, M., Croft, B., Ridley, D. A., McConnell, J. R., Sharma, S., Husain, L., Dutkiewicz, V. A., Eleftheriadis, K., Skov, H., and Hopke, P. K.: Multidecadal trends in aerosol radiative forcing over the Arctic: Contribution of changes in anthropogenic aerosol to Arctic warming since 1980, Journal of Geophysical Research: Atmospheres, 122, 3573-3594, https://doi.org/10.1002/2016JD025321, 2017.

Chen, M., and Zhuang, Q.: Evaluating aerosol direct radiative effects on global terrestrial ecosystem carbon dynamics from 2003 to 2010, Tellus Series B-Chemical and Physical Meteorology, 66, 10.3402/tellusb.v66.21808, 2014.

Cirino, G. G., Souza, R. A. F., Adams, D. K., and Artaxo, P.: The effect of atmospheric aerosol particles and clouds on net ecosystem exchange in the Amazon, Atmos Chem Phys, 14, 6523-6543, 10.5194/acp-14-6523-2014, 2014.

Cohan, D. S., Xu, J., Greenwald, R., Bergin, M. H., and Chameides, W. L.: Impact of atmospheric aerosol light scattering and absorption on terrestrial net primary productivity, Global Biogeochemical Cycles, 16, 10.1029/2001gb001441, 2002.

Doughty, C. E., Flanner, M. G., and Goulden, M. L.: Effect of smoke on subcanopy shaded light, canopy temperature, and carbon dioxide uptake in an Amazon rainforest, Global Biogeochemical Cycles, 24, 10.1029/2009gb003670, 2010.

Ezhova, E., Ylivinkka, I., Kuusk, J., Komsaare, K., Vana, M., Krasnova, A., Noe, S., Arshinov, M., Belan, B., Park, S. B., Lavric, J. V., Heimann, M., Petaja, T., Vesala, T., Mammarella, I., Kolari, P., Back, J., Rannik, U., Kerminen, V. M., and Kulmala, M.: Direct effect of aerosols on solar radiation and gross primary production in boreal and hemiboreal forests, Atmos Chem Phys, 18, 17863-17881, 10.5194/acp-18-17863-2018, 2018.

Farquhar, G. D., Caemmerer, S. V., and Berry, J. A.: A biochemical-model of photosynthetic CO2 assimilation in leaves of C-3 species, Planta, 149, 78-90, 10.1007/bf00386231, 1980.

Fisher, J. A., Jacob, D. J., Wang, Q., Bahreini, R., Carouge, C. C., Cubison, M. J., Dibb, J. E., Diehl, T., Jimenez, J. L., Leibensperger, E. M., Lu, Z., Meinders, M. B. J., Pye, H. O. T., Quinn, P. K., Sharma, S., Streets, D. G., van Donkelaar, A., and Yantosca, R. M.: Sources, distribution, and acidity of sulfate–ammonium aerosol in the Arctic in winter–spring, Atmos Environ, 45, 7301-7318,

https://doi.org/10.1016/j.atmosenv.2011.08.030, 2011.

Friedlingstein, P., O'Sullivan, M., Jones, M. W., Andrew, R. M., Hauck, J., Olsen, A., Peters, G. P., Peters, W., Pongratz, J., Sitch, S., Le Quere, C., Canadell, J. G., Ciais, P., Jackson, R. B., Alin, S., Aragao, L. E. O. C., Arneth, A., Arora, V., Bates, N. R., Becker, M., Benoit-Cattin, A., Bittig, H. C., Bopp, L., Bultan, S., Chandra, N., Chevallier, F., Chini, L. P., Evans, W., Florentie, L., Forster, P. M., Gasser, T., Gehlen, M., Gilfillan, D., Gkritzalis, T., Gregor, L., Gruber, N., Harris, I., Hartung, K., Haverd, V., Houghton, R. A., Ilyina, T., Jain, A. K., Joetzjer, E., Kadono, K., Kato, E., Kitidis, V., Korsbakken, J. I., Landschutzer, P., Lefevre, N., Lenton, A., Lienert, S., Liu, Z., Lombardozzi, D., Marland, G., Metzl, N., Munro, D. R., Nabel, J. E. M. S., Nakaoka, S.-I., Niwa, Y., O'Brien, K., Ono, T., Palmer, P. I., Pierrot, D., Poulter, B., Resplandy, L., Robertson, E., Rodenbeck, C., Schwinger, J., Seferian, R., Skjelvan, I., Smith, A. J. P., Sutton, A. J., Tanhua, T., Tans, P. P., Tian, H., Tilbrook, B., Van der Werf, G., Vuichard, N., Walker, A. P., Wanninkhof, R., Watson, A. J., Willis, D., Wiltshire, A. J., Yuan, W., Yue, X., and Zaehle, S.: Global Carbon Budget 2020, Earth System Science Data, 12, 3269-3340, 10.5194/essd-12-3269-2020, 2020.

Giorgi, F., Coppola, E., Solmon, F., Mariotti, L., Sylla, M. B., Bi, X., Elguindi, N., Diro, G. T., Nair, V., Giuliani, G., Turuncoglu, U. U., Cozzini, S., Guttler, I., O'Brien, T. A., Tawfik, A. B., Shalaby, A., Zakey, A. S., Steiner, A. L., Stordal, F., Sloan, L. C., and Brankovic, C.: RegCM4: model description and preliminary tests over multiple CORDEX domains, Climate Research, 52, 7-29, 10.3354/cr01018, 2012.

Gu, L. H., Baldocchi, D., Verma, S. B., Black, T. A., Vesala, T., Falge, E. M., and Dowty, P. R.: Advantages of diffuse radiation for terrestrial ecosystem productivity, J Geophys Res-Atmos, 107, 10.1029/2001jd001242, 2002.

Gu, L. H., Baldocchi, D. D., Wofsy, S. C., Munger, J. W., Michalsky, J. J., Urbanski, S. P., and Boden, T. A.: Response of a deciduous forest to the Mount Pinatubo eruption: Enhanced photosynthesis, Science, 299, 2035-2038, 10.1126/science.1078366, 2003.

Guenther, A. B., Jiang, X., Heald, C. L., Sakulyanontvittaya, T., Duhl, T., Emmons, L. K., and Wang, X.: The Model of Emissions of Gases and Aerosols from Nature version 2.1 (MEGAN2.1): an extended and updated framework for modeling biogenic emissions, Geosci. Model Dev., 5, 1471-1492, 10.5194/gmd-5-1471-2012, 2012.

He, M. Z., Ju, W. M., Zhou, Y. L., Chen, J. M., He, H. L., Wang, S. Q., Wang, H. M., Guan, D. X., Yan, J. H., Li, Y. N., Hao, Y. B., and Zhao, F. H.: Development of a two-leaf light use efficiency model for improving the calculation of terrestrial gross primary productivity, Agricultural and Forest Meteorology, 173, 28-39, 10.1016/j.agrformet.2013.01.003, 2013.

Hemes, K. S., Verfaillie, J., and Baldocchi, D. D.: Wildfire-Smoke Aerosols Lead to Increased Light Use Efficiency Among Agricultural and Restored Wetland Land Uses in California's Central Valley, Journal of Geophysical Research-Biogeosciences, 125, 21, 10.1029/2019jg005380, 2020.

Hoesly, R. M., Smith, S. J., Feng, L., Klimont, Z., Janssens-Maenhout, G., Pitkanen, T., Seibert, J. J., Linh, V., Andres, R. J., Bolt, R. M., Bond, T. C., Dawidowski, L., Kholod, N., Kurokawa, J.-i., Li, M., Liu, L., Lu, Z., Moura, M. C. P., O'Rourke, P. R., and Zhang, Q.: Historical (1750-2014) anthropogenic emissions of reactive gases and aerosols from the Community Emissions Data System (CEDS), Geosci Model Dev, 11, 369-408, 10.5194/gmd-11-369-2018, 2018.

Jaeglé, L., Quinn, P. K., Bates, T. S., Alexander, B., and Lin, J. T.: Global distribution of sea salt aerosols: new constraints from in situ and remote sensing observations, Atmos. Chem. Phys., 11, 3137-3157, 10.5194/acp-11-3137-2011, 2011.

Jing, X., Huang, J., Wang, G., Higuchi, K., Bi, J., Sun, Y., Yu, H., and Wang, T.: The effects of clouds and aerosols on net ecosystem CO2 exchange over semi-arid Loess Plateau of Northwest China, Atmos

Chem Phys, 10, 8205-8218, 10.5194/acp-10-8205-2010, 2010.

Kanniah, K. D., Beringer, J., and Hurley, L.: Exploring the link between clouds, radiation, and canopy productivity of tropical savannas, Agricultural and Forest Meteorology, 182, 304-313, 10.1016/j.agrformet.2013.06.010, 2013.

Keppel-Aleks, G., and Washenfelder, R. A.: The effect of atmospheric sulfate reductions on diffuse radiation and photosynthesis in the United States during 1995-2013, Geophys Res Lett, 43, 9984-9993, 10.1002/2016gl070052, 2016.

Kinne, S.: Aerosol radiative effects with MACv2, Atmos. Chem. Phys., 19, 10919-10959, 10.5194/acp-19-10919-2019, 2019.

Kvalevåg, M. M., and Myhre, G.: Human Impact on Direct and Diffuse Solar Radiation during the Industrial Era, Journal of Climate, 20, 4874-4883, 10.1175/jcli4277.1, 2007.

Li, X., and Xiao, J.: Mapping Photosynthesis Solely from Solar-Induced Chlorophyll Fluorescence: A Global, Fine-Resolution Dataset of Gross Primary Production Derived from OCO-2, Remote Sensing, 11, 10.3390/rs11212563, 2019.

Lu, X., Chen, M., Liu, Y., Miralles, D. G., and Wang, F.: Enhanced water use efficiency in global terrestrial ecosystems under increasing aerosol loadings, Agricultural and Forest Meteorology, 237, 39-49, 10.1016/j.agrformet.2017.02.002, 2017.

Malavelle, F. F., Haywood, J. M., Mercado, L. M., Folberth, G. A., Bellouin, N., Sitch, S., and Artaxo, P.: Studying the impact of biomass burning aerosol radiative and climate effects on the Amazon rainforest productivity with an Earth system model, Atmos Chem Phys, 19, 1301-1326, 10.5194/acp-19-1301-2019, 2019.

Matsui, T., Beltran-Przekurat, A., Niyogi, D., Pielke, R. A., Sr., and Coughenour, M.: Aerosol light scattering effect on terrestrial plant productivity and energy fluxes over the eastern United States, J Geophys Res-Atmos, 113, 10.1029/2007jd009658, 2008.

Mercado, L. M., Bellouin, N., Sitch, S., Boucher, O., Huntingford, C., Wild, M., and Cox, P. M.: Impact of changes in diffuse radiation on the global land carbon sink, Nature, 458, 1014-U1087, 10.1038/nature07949, 2009.

Moreira, D. S., Longo, K. M., Freitas, S. R., Yamasoe, M. A., Mercado, L. M., Rosario, N. E., Gloor, E., Viana, R. S. M., Miller, J. B., Gatti, L. V., Wiedemann, K. T., Domingues, L. K. G., and Correia, C. C. S.: Modeling the radiative effects of biomass burning aerosols on carbon fluxes in the Amazon region, Atmos Chem Phys, 17, 14785-14810, 10.5194/acp-17-14785-2017, 2017.

Paulot, F., Paynter, D., Ginoux, P., Naik, V., and Horowitz, L. W.: Changes in the aerosol direct radiative forcing from 2001 to 2015: observational constraints and regional mechanisms, Atmos. Chem. Phys., 18, 13265-13281, 10.5194/acp-18-13265-2018, 2018.

Rap, A., Spracklen, D. V., Mercado, L., Reddington, C. L., Haywood, J. M., Ellis, R. J., Phillips, O. L., Artaxo, P., Bonal, D., Coupe, N. R., and Butt, N.: Fires increase Amazon forest productivity through increases in diffuse radiation, Geophys Res Lett, 42, 4654-4662, 10.1002/2015gl063719, 2015.

Rap, A., Scott, C. E., Reddington, C. L., Mercado, L., Ellis, R. J., Garraway, S., Evans, M. J., Beerling, D. J., MacKenzie, A. R., Hewitt, C. N., and Spracklen, D. V.: Enhanced global primary production by biogenic aerosol via diffuse radiation fertilization, Nature Geoscience, 11, 640-+, 10.1038/s41561-018-0208-3, 2018.

Roderick, M. L., Farquhar, G. D., Berry, S. L., and Noble, I. R.: On the direct effect of clouds and atmospheric particles on the productivity and structure of vegetation, Oecologia, 129, 21-30, 10.1007/s004420100760, 2001.

Spitters, C. J. T., Toussaint, H., and Goudriaan, J.: Separating the diffuse and direct component of global radiation and its implications for modeling canopy photosynthesis Part 1. components of incoming radiation, Agricultural and Forest Meteorology, 38, 217-229, 10.1016/0168-1923(86)90060-2, 1986.

Strada, S., Unger, N., and Yue, X.: Observed aerosol-induced radiative effect on plant productivity in the eastern United States, Atmos Environ, 122, 463-476, 10.1016/j.atmosenv.2015.09.051, 2015.

Strada, S., and Unger, N.: Potential sensitivity of photosynthesis and isoprene emission to direct radiative effects of atmospheric aerosol pollution, Atmos Chem Phys, 16, 4213-4234, 10.5194/acp-16-4213-2016, 2016.

Wang, B., Wang, Z., Wang, C., Wang, X., Li, J., Jia, Z., Li, P., Wu, J., Chen, M., and Liu, L.: Field evidence reveals conservative water use of poplar saplings under high aerosol conditions, Journal of Ecology, 109, 2190-2202, https://doi.org/10.1111/1365-2745.13633, 2021.

Wang, X., Wu, J., Chen, M., Xu, X., Wang, Z., Wang, B., Wang, C., Piao, S., Lin, W., Miao, G., Deng, M., Qiao, C., Wang, J., Xu, S., and Liu, L.: Field evidences for the positive effects of aerosols on tree growth, Global Change Biology, 24, 4983-4992, 10.1111/gcb.14339, 2018.

Xie, X., Wang, T., Yue, X., Li, S., Zhuang, B., and Wang, M.: Effects of atmospheric aerosols on terrestrial carbon fluxes and CO2 concentrations in China, Atmos Res, 237, 10.1016/j.atmosres.2020.104859, 2020.

Yu, H., Kaufman, Y. J., Chin, M., Feingold, G., Remer, L. A., Anderson, T. L., Balkanski, Y., Bellouin, N., Boucher, O., Christopher, S., DeCola, P., Kahn, R., Koch, D., Loeb, N., Reddy, M. S., Schulz, M., Takemura, T., and Zhou, M.: A review of measurement-based assessments of the aerosol direct radiative effect and forcing, Atmos Chem Phys, 6, 613-666, 10.5194/acp-6-613-2006, 2006.

Yue, X., Wang, H. J., Liao, H., and Fan, K.: Simulation of dust aerosol radiative feedback using the GMOD: 2. Dust-climate interactions, J Geophys Res-Atmos, 115, 10.1029/2009jd012063, 2010.

Yue, X., and Liao, H.: Climatic responses to the shortwave and longwave direct radiative effects of sea salt aerosol in present day and the last glacial maximum, Climate Dynamics, 39, 3019-3040, 10.1007/s00382-012-1312-5, 2012.

Yue, X., and Unger, N.: The Yale Interactive terrestrial Biosphere model version 1.0: description, evaluation and implementation into NASA GISS ModelE2, Geosci Model Dev, 8, 2399-2417, 10.5194/gmd-8-2399-2015, 2015.

Yue, X., Unger, N., and Zheng, Y.: Distinguishing the drivers of trends in land carbon fluxes and plant volatile emissions over the past 3 decades, Atmos Chem Phys, 15, 11931-11948, 10.5194/acp-15-11931-2015, 2015.

Yue, X., Strada, S., Unger, N., and Wang, A.: Future inhibition of ecosystem productivity by increasing wildfire pollution over boreal North America, Atmos Chem Phys, 17, 13699-13719, 10.5194/acp-17-13699-2017, 2017.

Yue, X., and Unger, N.: Aerosol optical depth thresholds as a tool to assess diffuse radiation fertilization of the land carbon uptake in China, Atmos Chem Phys, 17, 1329-1342, 10.5194/acp-17-1329-2017, 2017.

Yue, X., and Unger, N.: Fire air pollution reduces global terrestrial productivity, Nature Communications, 9, 10.1038/s41467-018-07921-4, 2018.

Zhou, H., Yue, X., Lei, Y., Tian, C., Ma, Y., and Cao, Y.: Aerosol radiative and climatic effects on ecosystem productivity and evapotranspiration, Current Opinion in Environmental Science & Health, 19, 100218, 10.1016/j.coesh.2020.10.006, 2021a.

Zhou, H., Yue, X., Lei, Y., Tian, C., Ma, Y., and Cao, Y.: Large contributions of diffuse radiation to global gross primary productivity during 1981-2015, Global Biogeochemical Cycles,

https://doi.org/10.5194/acp-2021-701
Preprint. Discussion started: 16 September 2021

https://doi.org/10.1029/2021GB006957, 2021b.

Zhou, H., Yue, X., Lei, Y., Zhang, T., Tian, C., Ma, Y., and Cao, Y.: Responses of gross primary productivity to diffuse radiation at global FLUXNET sites, Atmos Environ, 244, 117905, 10.1016/j.atmosenv.2020.117905, 2021c.

Zhu, P. Y., Cheng, S. J., Butterfield, Z., Keppel-Aleks, G., and Steiner, A. L.: The Global Influence of Cloud Optical Thickness on Terrestrial Carbon Uptake, Earth Interact., 23, 22, 10.1175/ei-d-17-0035.1, 2019.

https://doi.org/10.5194/acp-2021-701
Preprint. Discussion started: 16 September 2021

Table 1 Summary of previous studies about aerosol DFE

Period	Region	Method	Species	Results[a]	References
2000-2001	Eastern United States	Model	Aerosols	Aerosol DFE decreases NPP by 0.71 g C m^{-2} (-0.09%) in 2000 but increases NPP by 5 g C m^{-2} (0.5%) in 2001	Matsui et al. (2008)
1960-1999	Global	Model	Cloud and aerosols	DFE enhances the land carbon sink by approximately one quarter during 1960-1999	Mercado et al. (2009)
2002-2003	Amazon	Flux.obs	Smoke aerosols	The increase of CO_2 uptake under high AOD is due to DFE (80%) and decreased temperature (20%)	Doughty et al. (2010)
2007 July–August	Northwest China	Flux.obs	Cloud and aerosols	Cloud dominates DFE, but aerosols lead to negative carbon uptake	Jing et al. (2010)
2003-2010	Global	Model	Aerosols	Aerosol DFE enhances GPP by 4.9 Pg C yr^{-2}, NPP by 3.8 Pg C yr^{-2}, and NEP by 3.9 Pg C yr^{-2}	Chen and Zhuang (2014)
1999-2009	Amazon	Flux.obs	Cloud and fire aerosols	Low AOD and cloud cover lead to relatively larger photosynthetic efficiency than high aerosol loading and thick cloud	Cirino et al. (2014)
1998-2007	Amazon	Model	Fire aerosols	Fire aerosols enhance diffuse radiation by 3.4-6.8% and NPP by 1.4-2.8%	Rap et al. (2015)
2003-2012	Eastern United States	Flux.obs	Aerosols	High AOD (>0.6) enhances plant productivity for forests, but causes negative effects for croplands and grasslands.	Strada et al. (2015)
2000	Global	Model	Aerosols	Aerosol DFE increases global GPP by 1-2%	Strada and Unger (2016)
1995-2013	United States	Model	Sulfate aerosols	The reductions of sulfate aerosols lead to decreased diffuse light by 0.6% yr^{-1} and GPP by 0.07% yr^{-1}	Keppel-Aleks and Washenfelder (2016)
2010	Amazon	Model	Fire aerosols	Fire aerosols increase GPP by 27%, plant respiration by 10% and decrease soil respiration by 3%	Moreira et al. (2017)
2010 2050	Boreal North America	Model	Fire aerosols	Fire aerosols increase NPP by 8 Tg C yr^{-1} at 2010s and 14 Tg C yr^{-1} at 2050s due to increased diffuse radiation of 2.6 W m^{-2} (1.7%) and 4.0 W m^{-2} (2.3%)	Yue et al. (2017)
2009-2011	China	Model	Aerosols	Aerosols increase NPP by 1.6±0.5% at all-sky and 35±0.9% at clear-sky	Yue and Unger (2017)

https://doi.org/10.5194/acp-2021-701
Preprint. Discussion started: 16 September 2021

2008-2017	Eurasia	Flux.obs	Aerosols	High aerosol loading increases GPP by 6-14% at all sites.	Ezhova et al. (2018)
2000	Global	Model	Biogenic aerosols	Biogenic aerosols enhance global NPP by 1.23 Pg C yr^{-1} due to DFE	Rap et al. (2018)
2001-2011	Global	Model	All and fire aerosols	All (fire) aerosols increase global GPP by 1.0±0.2 (0.05±0.3) Pg C yr^{-1} due to DFE	Yue and Unger (2018)
2014-2015	China	Flux.obs	Aerosols	Photosynthesis of sunlit and shaded leaves increases by 0.56% and 10.71% due to the increase AOD of 0.1	Wang et al. (2018)
2000	Amazon	Model	Fire aerosols	Fire aerosols increase NPP by 5-13 Tg C yr^{-1} due to radiative effects	Malavelle et al. (2019)
2018	Western North America	Flux.obs	Wildfire-smoke aerosols	Aerosols lead to GPP enhancement of 1.2-4.1% compared to the previous growing season	Hemes et al. (2020)
2006-2015	China	Model	Aerosols	Aerosols enhance GPP by 0.36 Pg C yr^{-1} (5%), and DFE makes the dominant contribution (59-62%)	Xie et al. (2020)

[a] Carbon metrics include net primary productivity (NPP), net ecosystem productivity (NEP) and gross primary productivity (GPP)

https://doi.org/10.5194/acp-2021-701
Preprint. Discussion started: 16 September 2021

Atmospheric Chemistry and Physics Discussions

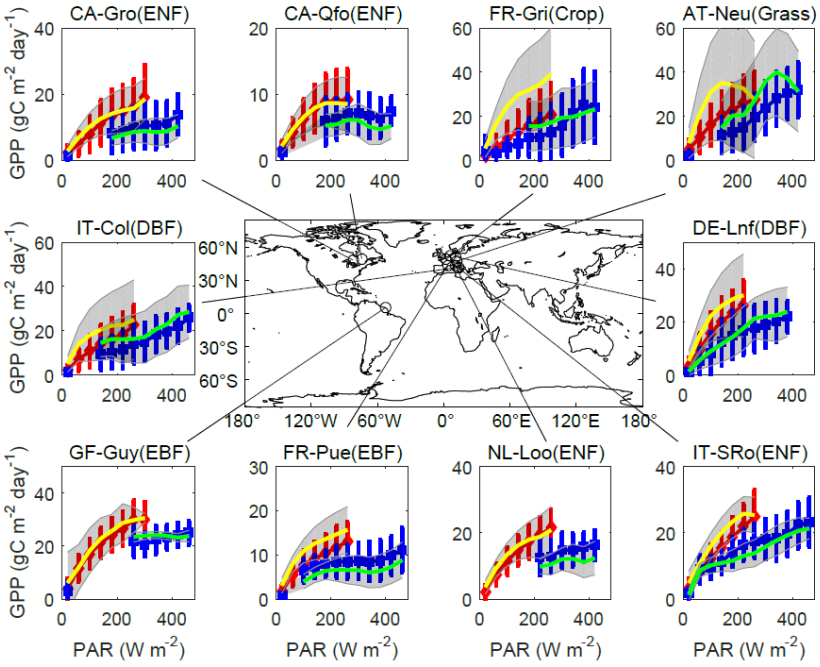

Figure 1 Simulated and observed GPP responses to direct and diffuse radiation. The comparisons are performed at 10 FLUXNET sites where more than 8 years of observations are available. For each site, hourly observations are divided into direct and diffuse conditions if diffuse fraction is <0.2 (blue squares) and >0.8 (red diamonds), respectively. The classified observations are averaged over PAR bins of 40 W m $^{-2}$ with errorbars indicating one standard deviation of GPP for each bin. Similarly, simulations are also divided into direct (green) and diffuse (yellow) bins of PAR with gray shading indicating one standard deviation. The plant function types include evergreen broadleaf forest (EBF), evergreen needleleaf forest (ENF), deciduous broadleaf forest (DBF), grassland (Grass), and cropland (Crop). The site name and vegetation type are listed on the title of each panel.

https://doi.org/10.5194/acp-2021-701
Preprint. Discussion started: 16 September 2021

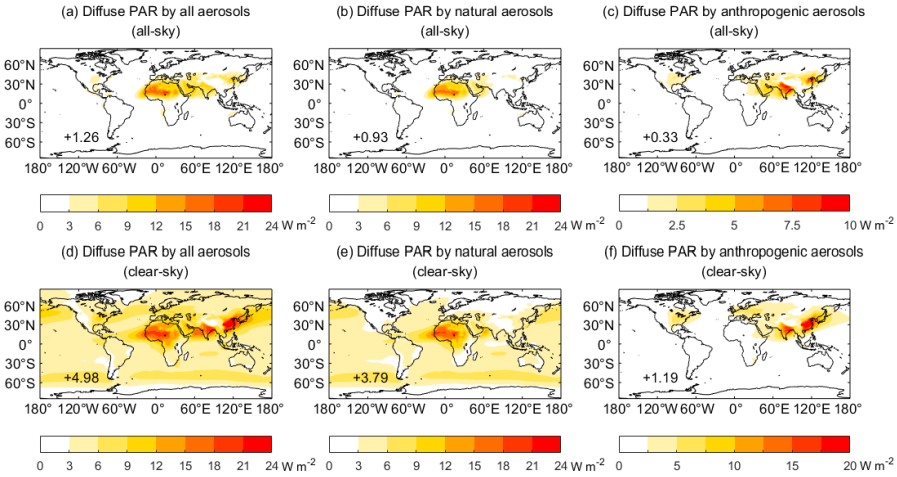

Figure 2 Global changes of diffuse PAR at surface by all, natural, and anthropogenic aerosols at all skies (a, b, c) and clear skies (d, e, f). The aerosol species include natural (BC, OC, dust, sea salt, sulfate, and nitrate) and anthropogenic (BC, OC, sulfate, and nitrate) aerosols. The total changes in PAR caused by different aerosol sources are shown on corresponding panels. Changes of diffuse PAR caused by individual aerosol species can be seen in Fig. S4. The units are W m^{-2}.

https://doi.org/10.5194/acp-2021-701
Preprint. Discussion started: 16 September 2021

Atmospheric Chemistry and Physics Discussions
Open Access

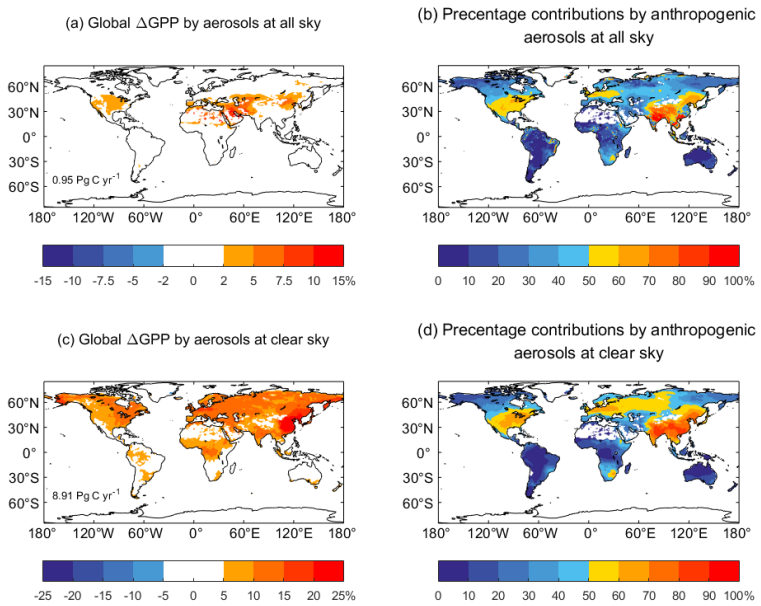

Figure 3 Percentage changes in GPP caused by aerosol diffuse fertilization effect and percentage contributions by anthropogenic aerosols at (a, b) all skies and (c, d) clear skies. The DFE of all aerosols (natural + anthropogenic) are shown on the left, and the contributions by anthropogenic aerosols alone are shown on the right.

https://doi.org/10.5194/acp-2021-701
Preprint. Discussion started: 16 September 2021

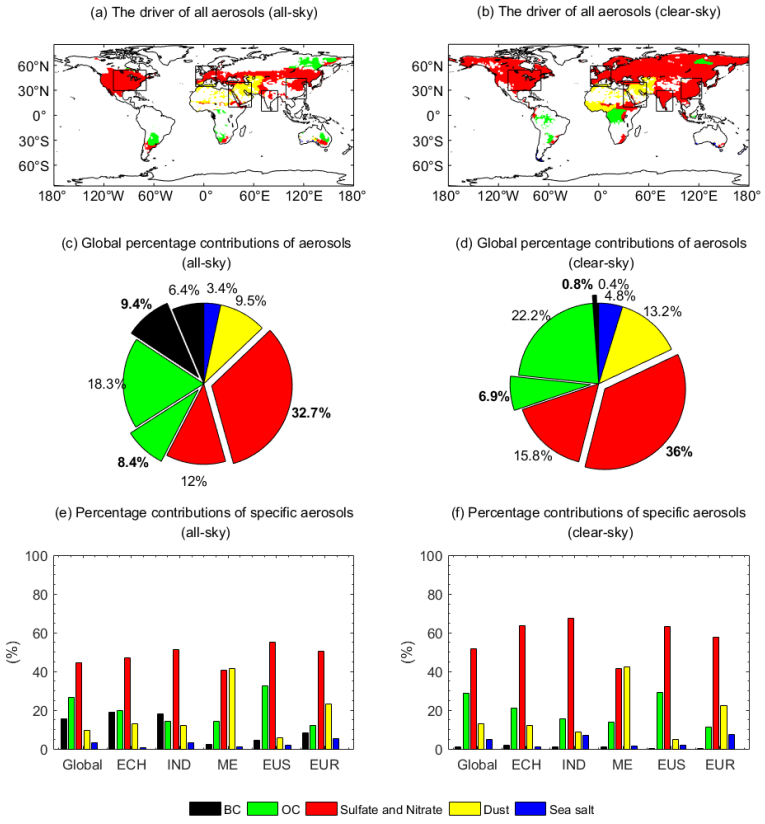

Figure 4 (a, b) Dominant aerosol species contributing to the simulated changes in GPP and the percentage contributions of aerosol species for global (c, d) and specific regions (e, f) at (a, c, e) all skies and (b, d, f) clear skies. The contributions in (c, e) and (d, f) are calculated as the ratios of absolute DFE, as BC aerosols induce negative DFE. The normal (bold) fonts in (c) and (d) represent aerosol species from natural (anthropogenic) sources. Regions with relatively high percentage changes in GPP (>1% for all-sky and >5% for clear-sky) by aerosols are shown in Figure (a) and (b). The regions include eastern China (ECH), India (INA), Middle East (ME), eastern U.S. (EUS), and Europe (EUR), which are marked as black boxes in (a) and (b). The black, green, red, yellow, and blue represent the effects of BC, OC, sulfate and nitrate, dust, and sea salt aerosols, respectively.

https://doi.org/10.5194/acp-2021-701
Preprint. Discussion started: 16 September 2021

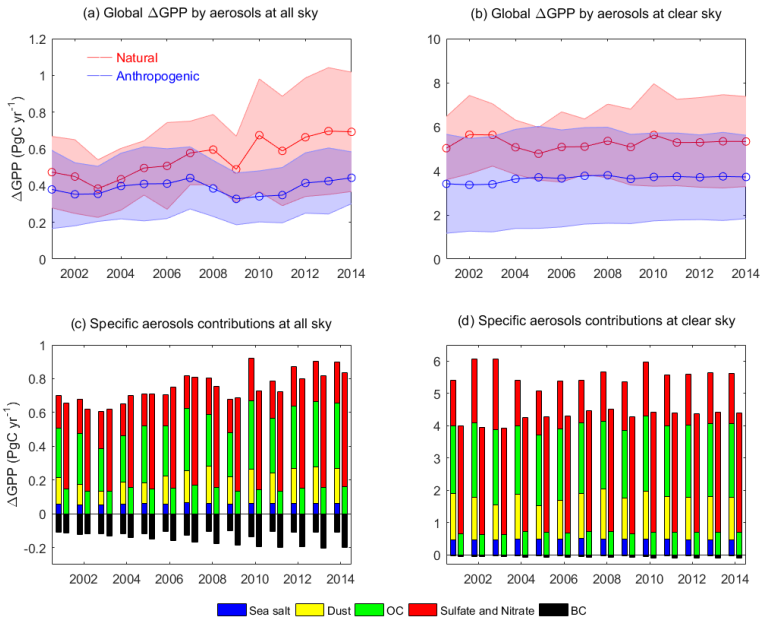

Figure 5 Interannual variations of GPP changes induced by the DFE of natural and anthropogenic aerosols at (a, c) all skies and (b, d) clear skies during 2001-2014. The left and right bars at each year in (c) and (d) represent the effects of natural and anthropogenic aerosol species, respectively. The hollow circles and shadings in (a) and (b) represent annual mean and standard deviation of aerosol-induced GPP changes. The black, green, red, yellow, and blue bars indicate the effects of BC, OC, sulfate and nitrate, dust, and sea salt aerosols, respectively.